Applied Catalysis A: General 392 (2011) 93-102

# Understanding the complexity of a catalyst synthesis: Co-precipitation of mixed Cu,Zn,Al hydroxycarbonate precursors for $Cu/ZnO/Al_2O_3$ catalysts investigated by titration experiments

M. Behrens,*[,a] D. Brennecke,[a] F. Girgsdies,[a] S. Kißner,[a] A. Trunschke,[a] N. Nasrudin,[b] S. Zakaria,[c] N. Fadilah Idris,[c] S. B. Abd Hamid,[b] B. Kniep,[d] R. Fischer,[d] W. Busser,[e] M. Muhler,[e] R. Schlögl[a]

[a]Fritz-Haber-Institute of the Max-Planck-Society, Department of Inorganic Chemistry, Faradayweg 4-6, 14195 Berlin, Germany
[b]Combinatorial Technology and Catalyst Research Centre (COMBICAT), University of Malaya, 50603, Kuala Lumpur, Malaysia
[c]NanoC Sdn Bhd, No. 29, Jln PJU 3/47, Seksyen PJU 3, Sunway Technology Park, 47810 Petaling Jaya, Sengalor, Malaysia
[d]Süd-Chemie AG, Catlysts Research & Development, Waldheimer Str. 13, 83052 Bruckmühl, Germany.
[e]Ruhr-University Bochum, Industrial Chemistry, Universitätsstraße 150, 44801 Bochum, Germany

* Corresponding author: e-mail behrens@fhi-berlin.mpg.de,

Received 11 August 2010; Revised 27 October 2010; Available online 4 November 2010; Published 29 January 2011

**Abstract**

Co-precipitation of CuZn(Al) precursor materials is the traditional way of synthesizing $Cu/ZnO/(Al_2O_3)$ catalysts for industrial methanol synthesis. This process has been investigated by titration experiments of nitrate and formate solutions. It was found that the solidification of the single components proceeds sequentially in case of nitrates: $Cu^{2+}$ is precipitated at pH 3 and $Zn^{2+}$ (as well as $Al^{3+}$) near pH 5. This behavior prevents a homogeneous distribution of all metal species in the initial precipitate upon gradual increase of pH and requires application of the constant pH micro-droplet method.

This effect is less pronounced if formate instead of nitrate is used as counter ion. This can be explained by the strong modification of the hydrolysis chemistry of the metal ions due to the presence of formate anions, which act as ligands and buffer.

A formate-derived $Cu/ZnO/Al_2O_3$ catalyst was more active in methanol synthesis compared to a nitrate-derived sample although the same crystallographic phases were present in the precursor after co-precipitation and ageing.

The effect of precipitation temperature was studied for the binary CuZn nitrate model system. Increasing the temperature of co-precipitation above 50 °C leads to down-shift of the precipitation pH of $Zn^{2+}$ by a full unit. Thus, in warm solutions more acidic conditions can be used for complete co-precipitation, while in cold solutions, some $Zn^{2+}$ may remain dissolved in the mother liquor at the same precipitation pH. The higher limit of temperature is given by the tendency of the initial Cu precipitate towards formation of CuO by oxolation. On the basis of these considerations, the empirically determined optimal pH and temperature conditions of the industrially applied synthesis can be rationalized.

**Keywords:** $Cu/ZnO/Al_2O_3$ catalyst, preparation, co-precipitation, precursor, methanol synthesis

## 1. Introduction

Co-precipitation is a standard preparation technique for catalyst precursors. By proper adjustment of the precipitation parameters the homogeneous distribution of different metal cations in a mixed solution can be carried over to a multinary catalyst precursor by rapid solidification [1]. Highly dispersed, well mixed and homogeneous

metal/oxide catalysts can be obtained from such precursors by decomposition and reduction. A prominent example is the co-precipitation of mixed Cu,Zn,Al hydroxycarbonates as precursor material for Cu/ZnO/$Al_2O_3$ catalysts which are employed for the industrial synthesis of methanol [2].

A common and technically relevant route of preparation starts from mixed solution of $Cu^{2+}$, $Zn^{2+}$ and $Al^{3+}$ salts and sodium carbonate as precipitating agent. Typical concentrations are around 1 M and an industrially applied composition is Cu:Zn:Al ~ 60:30:10. This synthesis route was shown to yield highly active catalysts, but is rather complex. The exact settings of the synthesis parameters during the co-precipitation step – especially pH and temperature – were shown to be of crucial importance for the catalytic properties of the final catalyst. These (and other) parameters have been studied mostly phenomenologically and their critical influence – termed the chemical memory of the CuZnAl system [3] – has been investigated for many years by different groups [3-9] and optimized settings for temperature and pH are documented in literature [8,9]. In a recent sophisticated parallel preparation and testing study a quantitative basis for the chemical memory was elaborated by Baltes et al. showing that enormous differences in catalytic activity are possible for the same nominal catalyst composition in the pH-temperature parameter field [10]. In agreement with previous reports, best conditions were reported for a temperature between 60 and 70 °C and for acidity and between pH 6 and 7.

The present study aims at contributing to the understanding of the effect of individual synthesis parameters during co-precipitation to help rationalizing this highly effective route of synthesis. More fundamental understanding might open the door for further and more rational optimization of this important catalyst system. We simulated the precipitation process of mixed Cu,Zn,Al precursors using increasing pH titration experiments. To better monitor the hydrolysis chemistry of the involved cations and their interplay, single metal salt solutions, the binary systems and the ternary Cu,Zn,Al system were investigated separately. Titration curves were recorded and samples of the precipitate were recovered at certain points of interest and subjected to powder X-ray diffraction analysis. UV-vis spectroscopy was applied to follow the $Cu^{2+}$ concentration in solution. The results directly relate to the increasing pH method of co-precipitation. Their relevance for the industrially applied constant pH co-precipitation method is discussed and the effect of precipitation temperature was studied for the binary nitrate model system.

In order to study the influence of counter anions, formates and nitrates have been chosen to represent systems with and without relevant contributions of the anions to acid-base chemistry. It is the scope of this study to investigate technically applied co-precipitation conditions for Cu/ZnO/$Al_2O_3$ catalyst precursors. Therefore, parameters like composition, temperature, and concentrations were chosen according to patented procedures for the nitrate [11] and the formate [12] route, respectively. Additionally to the titration experiments, the technically applied constant pH co-precipitation method was employed to compare the two precursor materials derived from nitrate and formate solutions.

We will discuss our results in context to the recently published [13] model for the chemical memory of the Cu,Zn system, which addresses the optimal setting of the Cu:Zn ratio and the role of the zincian malachite precursor phase. This model proposes a two-step microstructure-directing effect (meso-structuring during ageing and nano-structuring during calcination) as the key benefit of the technically applied route of preparation. The morphology of the precursor particles and the degree of Cu-substitution by Zn in the zincian malachite precursor phase were identified as the critical precursor properties determining the performance of the final catalyst.

## 2. Experimental

An automated laboratory titrator (Mettler Toledo Rondolino) was used for the titration experiments. The precipitating agent was aqueous $Na_2CO_3$ solution (1.6 M). For the metal nitrate solutions 108 mmol $Cu(NO_3)_2 \cdot 3\ H_2O$, 48 mmol ZnO or 22 mmol $Al(NO_3)_3 \cdot 9\ H_2O$ were immersed in low amounts of bi-distilled water and 12.5 ml of conc. nitric acid (65 wt.-%) were added. The mixture stirred at ca. 60 °C until all solid was dissolved. The solution was diluted to a total volume of 183 ml resulting in an overall concentration [$Cu^{2+}$+$Zn^{2+}$+$Al^{3+}$] of approximately 1 M. The same amounts of salts were combined to prepare the binary Cu,Zn and the ternary Cu,Zn,Al nitrate solution resulting in a molar Cu:Zn ratio of 71:29 for the former and a Cu:Zn:Al composition of 61:27:12 for the latter. In case of the metal formate solutions, appropriate amounts of $Cu_2(OH)_2CO_3$, ZnO and $Na_2Al_2O_4 \cdot 3\ H_2O$ were used as metal sources and 18.2 ml of conc. formic acid (85 wt.-%) were added to yield the same concentrations and compositions as in the nitrate solutions. During titrations the solutions were stirred using a magnetic stir bar and the rate of base addition was 1.6 ml/min. The temperature of the titration experiments was set to 65 °C and controlled by a water bath. For the binary Cu,Zn nitrate solution additional titration experiments were done at 30, 40, 50 and 60 °C with a base addition of 1.0 ml/min. For these experiments the acidity was adjusted to pH 0 at room temperature by addition of appropriate amounts of conc. nitric acid resulting in a slightly higher acidity compared to the nitrate experiments described above. The pH probe was carefully calibrated at each titration temperature directly before the experiment using commercial buffer solutions. Samples of the precipitates were taken at different points of interest, recovered by filtration and dried at 120 °C over night. No washing procedure was applied in order to minimize possible effects on the solids, resulting in the presence of sodium nitrate or formate peaks in some of the XRD patterns.

Catalyst preparation was performed by constant pH co-preciptiation in an automated laboratory reactor (Mettler-Toledo Labmax) at T = 65 °C from aqueous 1.6 M

$Na_2CO_3$ solution and 1 M aqueous metal nitrate or formate solution (prepared as described, Cu:Zn:Al = 61:27:12) at pH 6.5. The precipitate was aged for 3h in the mother liquor, filtrated, thoroughly washed with water and dried. The obtained bluish green precursor was calcined in air at 330 °C for 3h yielding poorly crystalline mixtures of the oxides.

Powder X-ray diffraction measurements were carried out on a STOE STADI P transmission diffractometer equipped with primary focusing Ge monochromator and linear position sensitive detector using $CuK\alpha_1$ radiation. Qualitative phase analysis was performed by comparison with reference patterns from the ICDD PDF2 database using the EVA [14] software. In some cases, further clarification of the phase composition was achieved by full pattern refinement according to the Rietveld method using the TOPAS [15] software and crystal structure data from the ICSD database. Furthermore, the Rietveld crystal structure refinement of a newly found phase was performed with TOPAS [15]. Cu domain sizes were determined from the FWHM of the Cu 111 line after calcination and reduction. Diffraction data of the freshly reduced material were recorded at room temperature (reduction in 2 vol.-% $H_2$ at 250 °C for 30 min) on a Bruker D8 Advance equipped with a high temperature chamber (Anton Paar). Thermogravimetric experiments were done on a NETZSCH Jupiter thermobalance in flowing air. IR spectra were recorded at room temperature with a FTIR Perkin-Elmer model 2000 using the ATR technique.

Catalytic testing was performed in a flow set-up equivalent to that described in ref. [16]. For fast on-line gas analysis, a calibrated quadrupole mass spectrometer (Pfeiffer Vacuum, Thermostar) was used. The following gases of high purity were used: He (99.9999 %), $H_2$ (99.9999 %), $N_2O$/He (1% N2O, 99.9995 %), $H_2$/He (2.0 % $H_2$, 99.9999%) and a mixture of 72% $H_2$, 10% CO, 4% $CO_2$ in He used as methanol synthesis feed gas (99.9995 %). A glass-lined stainless steel microreactor was filled with 100 mg catalyst (sieve fraction 250-355 µm). The catalyst was reduced by heating to 175 °C (1 K $min^{-1}$) in a gas mixture of 2.0 % $H_2$/He and subsequently in 100% $H_2$ to 240 °C. The catalytic activity under steady-state conditions was determined at 220°C and at 10 bar pressure, using a flow rate of 50 N ml $min^{-1}$. The copper surface area was determined applying $N_2O$ reactive frontal chromatography according to the method proposed by Chinchen et al. [17] at somewhat more moderate reaction conditions [16].

## 3. Results

A first titration experiment was conducted with the pure acids of a concentration applied for dissolution of the starting materials and acidification of the resulting solutions but without addition of metal salts (dotted lines in Figure 1). The titration curves reflect the under-lying neutralization reactions of formic and nitric acid. The nitrate route starts from a much more acidic solution of pH -0.5, whereas the starting pH of the formate route is around 1.

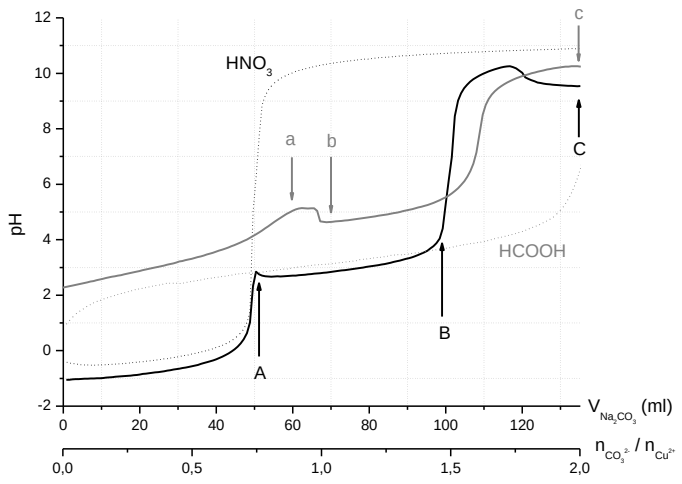


**Fig. 1:** Titration curves for the pure Cu solution, nitrate (black) and formate system (grey), letters denote points of sample recovery. Titration curves for the pure acids, nitric acid (black) and formic acid (grey) are shown as dotted lines.

The nitric acid curve has the typical S-shape for neutralization of strong acids. After the pH jump at the point of equivalence basicity does not exceed pH 11, which is due to the limited basic strength of the sodium carbonate solution. Formic acid as a medium strong acid is mostly undissociated and, due to its buffering effect towards incoming base (Scheme 1), a pH plateau around pH 3 can be observed in the titration curve.

$$HCOOH + OH^- \rightarrow HCOO^- + H_2O \quad (1)$$

As a consequence, more than double of the amount of base is necessary to reach pH 7 (usually applied in course of the co-precipitation using the constant pH method) compared to the nitrate route.

As expected, the titration curves are drastically changed by the presence of $Cu^{2+}$ (solid lines in Figure 1). The starting pH has further decreased to pH -1 for the nitrate route due to the additional acidity of hydrated $Cu^{2+}$ ions (Scheme 2).

$$[Cu(H_2O)_6]^{2+} \rightarrow [Cu(H_2O)_5(OH)]^+ + H^+ \quad (2)$$

After initially following the neutralization curve without formation of a precipitate, a solid started to form at a $[CO_3^{2-}]/[Cu^{2+}]$ ratio of 0.75. At this point a range of nearly constant pH sets in around pH 3 and lasts until a $[CO_3^{2-}]/[Cu^{2+}]$ ratio of 1.5 suggesting that incoming base is consumed for precipitation and does not contribute to the increase of pH of the solution in this region. Samples were recovered at the points marked with capital letters in Figure 1 and investigated by XRD (lower case letters are used for the formate system). The XRD patterns and phase identifications are presented as electronic supplementary data. In case of the Cu nitrate system, basic copper nitrate, gerhardtite $Cu_2(OH)_3NO_3$, could be identified by XRD as the only

crystalline phase in the blue precipitate at points *A* and *B* apart from some sodium nitrate (Figure S1, ESI). At point *B* no more $Cu^{2+}$ was found in the colorless filtrate by UV-vis spectroscopy indicating that that the plateau in pH represents the gradual consumption of $Cu^{2+}$ from the solution by formation of gerhardtite. Copper is completely solidified at pH > 4. At a $[CO_3^{2-}]/[Cu^{2+}]$ ratio of ca. 1.7 a decrease of pH is observed from approximately pH 10 down to pH 9. At point *C*, the precipitate turned dark and CuO was identified as an additional crystalline phase (Figure S1a, supplementary data) suggesting that the drop of pH is related to the formation of Cu oxide in basic environment [18], formally according to Scheme 3. Such a process of dehydration of a basic precipitate under formation of bridging oxygen atoms is called oxolation.

$$Cu_2(OH)_3(NO_3) + OH^- \rightarrow 2\ CuO + 2\ H_2O + NO_3^-. \qquad (3)$$

Gerhardtite was reported to transform into malachite, $Cu_2(OH)_2CO_3$, around pH 7 in course of a similar but slower titration experiment [19]. Here, only traces of malachite can be found with XRD, indicating that it is most likely due to the relatively fast addition of base that the formation of malachite is kinetically hindered.

In the formate case (Figure 1) the starting pH is slightly increased from pH ~ 1 for the pure aqueous acid to pH ~ 2 for the $Cu^{2+}$ containing solution owing to the partial neutralization of formic acid, which occurred already during dissolution of the basic copper carbonate salt. Initially, the pH increases almost linearly until near a $[CO_3^{2-}]/[Cu^{2+}]$ ratio of 0.9 a precipitate starts to form. Here, the titration curve exhibits a local maximum and a subsequent plateau around pH 5 until a $[CO_3^{2-}]/[Cu^{2+}]$ ratio of 1.6. At the end of the experiment pH 10 is reached. Three samples were taken at points *a*, *b* and *c* (Figure S1b, supplementary data). XRD shows the presence of a well crystalline phase at points *a* and *b*, which could not be identified as a known copper formate, carbonate or hydroxide phase by comparison with literature data. However, with the exception of a single peak at 10.37° 2θ (d = 8.52 Å), we were able to assign this pattern to the basic formate phase $Cu_2(OH)_3(HCOO)$, which probably corresponds to a phase mentioned in literature already in 1915 as "$Cu(HCOO)_2 \cdot 3\ Cu(OH)_2$" [20,21], but – to the best of our knowledge – has not been structurally characterized yet. It will be described in more detail below in section 4.2. After the complete titration at point *c* the compound has partially transformed to CuO by oxolation.

In case of the acidic Zn nitrate solution (pH -0.5), precipitation starts at a $[CO_3^{2-}]/[Zn^{2+}]$ ratio of 0.7 (Figure 2). As in case of Cu, a clear precipitation plateau is formed and the pH increases again at a $[CO_3^{2-}]/[Zn^{2+}]$ ratio 1.6 to finally reach pH 11 at the end of the experiment. The XRD patterns (Figure S2a, supplementary data) show a complex phase composition at points *A* and *B*, which is discussed in detail in the supplementary data. The diversity of crystalline phases documents a rich and dynamic chemistry of the Zn precipitate in the nitrate system. Oxolation is observed

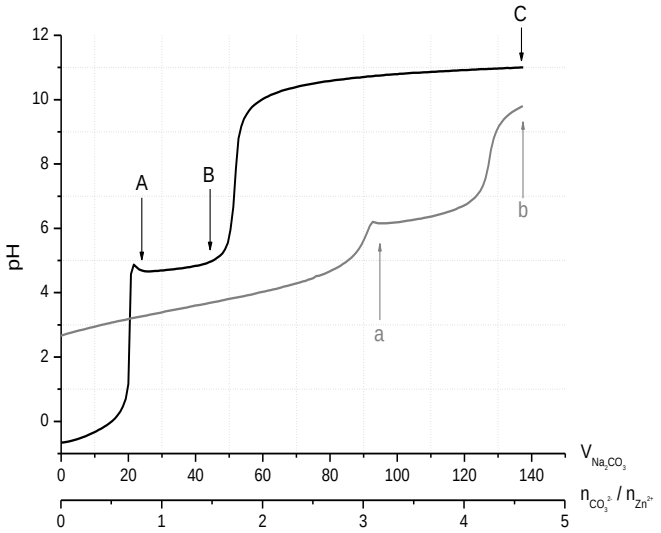


**Fig. 2:** Titration curves for the pure Zn solution, nitrate (black) and formate system (grey), letters denote points of sample recovery.

at lower pH compared to the copper system, but the formed ZnO seems to be reactive enough to react into other phases. The Zn formate system on the other hand does not precipitate until a $[CO_3^{2-}]/[Zn^{2+}]$ ratio of 3 is reached at a pH of 6 (Figure 2). The high background and broad peaks in the XRD pattern of the colorless solid recovered at point *a* is indicative of a generally poor crystallinity (Figure S2b, supplementary data), but some phases could be identified (see supplementary data).

Hydrolysis of $Al^{3+}$ solutions has been thoroughly investigated and many studies are documented in the literature. The typical general features of Al hydrolysis seem to be also present in our system, as is suggested by the similar shape of the titration curve shown in Figure 3 and the curves reported in literature [22,23]. The speciation of Al is complex and octahedral $[Al(H_2O)_6]^{3+}$ monomers transform under elimination of $H_3O^+$ into hydroxyl-bridged dimeric and oligomeric isopolyspecies upon addition of base. This condensation reaction of two water ligands into one bridging hydroxyl group is called olation. The exact course of $Al^{3+}$ hydrolysis, i.e. the nature and relative concentrations of soluble intermediate species as well as texture and crystallinity of the precipitate is known to critically depend on the exact process parameters like concentrations, nature of counter ions and precipitation agent, temperature, speed and method of base addition and ageing time [22-26]. A detailed investigation of these effects is beyond the scope of this paper. The olation process is associated with a plateau in the titration curve as incoming $OH^-$ is used as bridging ligand between $Al^{3+}$ centers and does not contribute to the increase of pH in this range. Olation is observed in our system between 3.7 and 4.8 for the $[CO_3^{2-}]/[Al^{3+}]$ ratios in the pH range 2.5 – 3.0. No precipitate is formed up to a $[CO_3^{2-}]/[Al^{3+}]$ ratio of 4.9 at pH 5, where a colorless X-ray amorphous solid was recovered. Only sodium nitrate was detected by XRD (Figure S3a, supplementary data). The pH of 11 at the end of the experiment is not high enough to

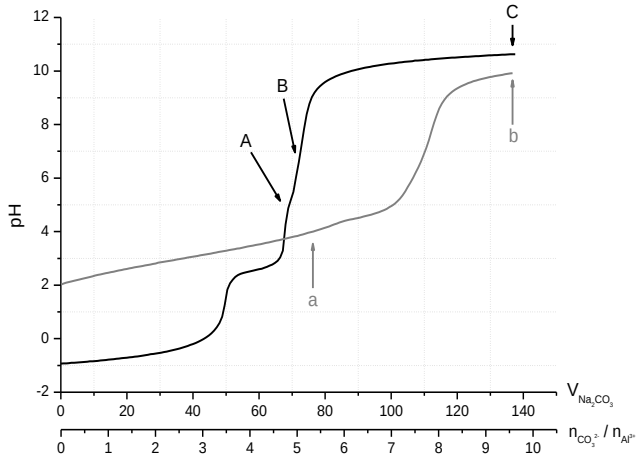


**Fig. 3:** Titration curves for the pure Al solution, nitrate (black) and formate system (grey), letters denote points of sample recovery

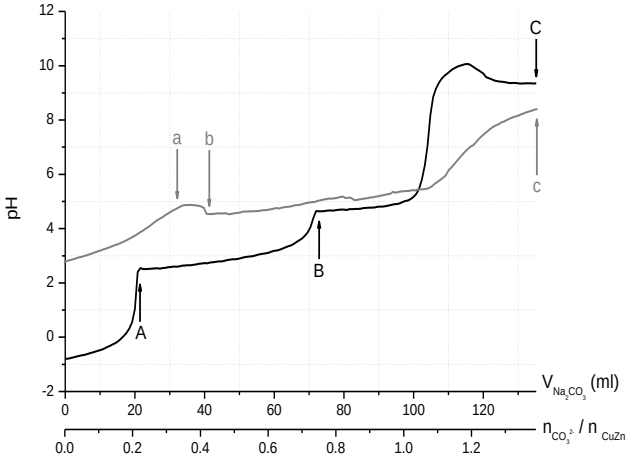


**Fig. 4:** Titration curves for the mixed Cu,Zn solution, nitrate system (black) and formate system (grey), letters denote points of sample recovery.

completely dissolve the precipitate in form of aluminate and the presence of dawsonite $NaAl(CO_3)(OH)_2$ in addition to sodium nitrate and the sodium carbonates $\gamma$-$Na_2CO_3$ and $Na_2CO_3 \cdot H_2O$ is observed by XRD after drying (Figure S3a, supplementary data). The titration curve of the Al formate system has a completely different shape. The pH increases nearly linearly until a $[CO_3^{2-}]/[Al^{3+}]$ ratio of 7 (Figure 3). At $[CO_3^{2-}]/[Al^{3+}] = 5$ a colorless and amorphous precipitate forms without causing any special feature in the pH curve. At the end of the experiment dawsonite is also present in the formate system (Figure S3b, supplementary data).

In the nitrate case, the titration curve of the binary Cu,Zn system can be considered as being composed from the features observed in the single metal salt systems (Figure 4). At pH 3 a plateau is observed due to gerhardtite formation ($0.2 < [CO_3^{2-}]/([Cu^{2+}]+[Zn^{2+}]) < 0.7$), which is the only crystalline solid present at points *A* and *B*. At point *B*, there is no more $Cu^{2+}$ detected in the filtrate by UV-vis spectroscopy indicating a complete solidification of copper. As in the pure Zn system, the precipitation of $Zn^{2+}$ is observed around pH 5 ($0.7 < [CO_3^{2-}]/([Cu^{2+}]+[Zn^{2+}]) < 1.1$). However, instead of pure zinc compounds a mixed binary aurichalcite-like phase $(Cu,Zn)_5(OH)_6(CO_3)_2$ is formed from the solidifying zinc and the freshly precipitated gerhardite as can be seen from the XRD pattern at point *C*, where a mixture of gerhardite and aurichalcite is present (Figure S4a, supplementary data). It is noted that the mineral hydrozincite $Zn_5(OH)_6(CO_3)_2$ crystallizes in a related crystal structure and exhibits a similar diffraction pattern like aurichalcite. The newly formed phase can be identified as aurichalcite by the presence of the 121 reflection near 32.8° 2θ, i.e. at a position, where no peak is present for hydrozinicte. However, the presence of minor amounts of hydrozincite cannot be excluded. Natural aurichalcite exhibits Cu/Zn ratios < 1. With respect to composition, a binary malachite-like phase, which is able to accommodate more Cu than Zn, should be favored for Cu-rich systems like ours. Malachite, $Cu_2(CO_3)(OH)_2$, can incorporate up to approximately 28 % Zn depending on the synthesis conditions [13] and is usually precipitated in its amorphous form (also called zincian georgeite [27]). It crystallizes only upon prolonged ageing of the fresh precipitate in the mother liquor [3,9,13]. Additional to this kinetical hindrance, another possible reason for the absence of (zincian) malachite may be the lowered reactivity of $Cu^{2+}$ due to the prior formation of gerhardite favoring the formation of Cu-poorer and structurally similar aurichalcite. Both phases are essentially built from layers of edge-sharing metal-oxygen octahedra. These related structural motifs might favor the crystallization of aurichalcite as a result of the reaction of freshly precipitated $Zn^{2+}$ and gerhardite. Accordingly, at the end of the titration gerhardite is completely consumed and transformed into a mixture of aurichalcite and CuO. The latter phase can be assumed to have formed from residual gerhardite by oxolation at high pH analogously to the titration of the pure Cu nitrate solution according to scheme (3).

A pronounced step-like shape of the titration curve is not observed for the Cu,Zn formate system (Figure 4). After the initial increase of pH, formation of a precipitate is observed at a $[CO_3^{2-}]/([Cu^{2+}]+[Zn^{2+}])$ ratio of 0.3. At this point a local maximum of pH is followed by a plateau around pH 5 lasting until $[CO_3^{2-}]/([Cu^{2+}]+[Zn^{2+}]) = 1.1$. XRD patterns of the sample collected at points *a* and *b* evidence formation of the hitherto unknown crystalline basic formate, which was already observed in the single Cu formate system (Figure S4b, supplementary data).

In the ternary system, the step-like titration curve of the nitrate system again reflects the sequential precipitation of the $Cu^{2+}$ and $Zn^{2+}$ species at pH 3 and 5, respectively (Figure 5). The onset of Cu precipitation at pH 2.5 – 3 falls into a range, where the olation of $Al^{3+}$ was observed in the single Al nitrate system. The superimposition of $Al^{3+}$ olation and onset of gerhardite precipitation might explain the smoother pH evolution near $[CO_3^{2-}]/([Cu^{2+}]+[Zn^{2+}]) = 0.3$ compared to the binary nitrate system. Furthermore, the presence of $Al^{3+}$ leads to formation of a hydrotalcite-like

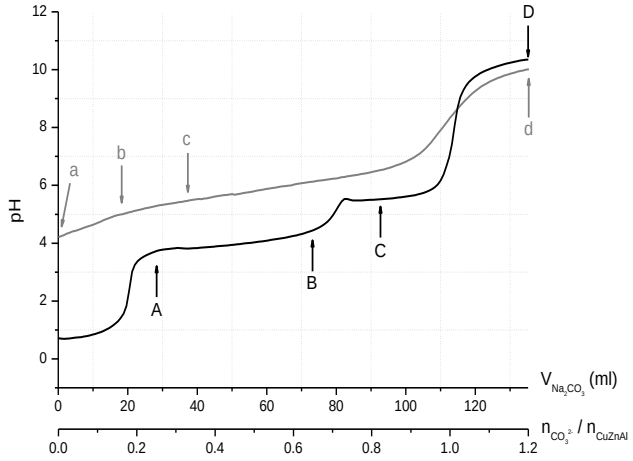


**Fig. 5:** Titration curves for the mixed Cu,Zn,Al solution, nitrate (black) and formate system (grey), letters denote points of sample recovery.

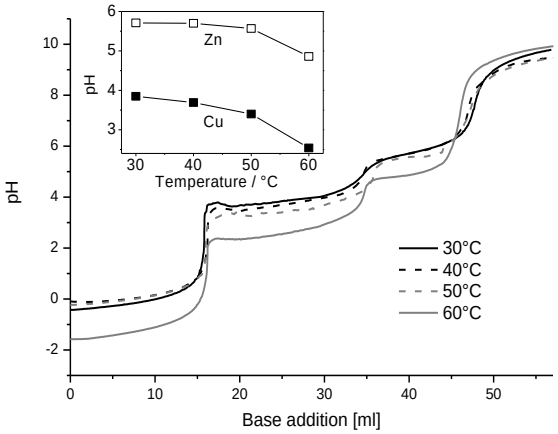


**Fig. 6:** Titration curves of the binary CuZn nitrate system recorded at different temperatures and precipitation pH of $Cu^{2+}$ and $Zn^{2+}$ determined after addition of 25 and 40 ml base, respectively (inset).

$(Cu,Zn)_{1-x}Al_x(OH)_2(CO_3)_{x/2}{\cdot}m\ H_2O$ phase at high pH (Figure S5a, supplementary data). A detailed discussion of the XRD results is given as supplementary data.

In the formate system, no clear solution was obtained at the beginning of the titration experiment. Instead, a colorless solid was observed to be suspended in the blue solution. The solid was recovered and identified as a mixture of zinc formate hydrate and bayerite (Figure S5b, supplementary data). The high initial pH of > 4 indicates that the solution is not acidic enough to dissolve all solid. The main reason is the use of basic sodium aluminate as Al source in order to exclude the presence of nitrate in the formate system. The titration curve of the ternary formate system is relatively smooth (Figure 5). Precipitation of a bluish green solid starts at pH 5 at a $[CO_3^{2-}]/([Cu^{2+}]+[Zn^{2+}]+[Al^{3+}])$ ratio between 0.1 and 0.2 without any sharp feature in the pH curve. At a ratio of 0.9 the system approaches the carbonate buffer regime and the curve resembles the neutralization curve shown in Figure 1, dotted lines, indicating the precipitation is complete at this point. A plethora of precipitate phases is observed by XRD during the titration experiment (Figure S5b, supplementary data) and details can be found in the supplementary data.

The effect of temperature was studied on the binary nitrate model system. The precipitation titration curves of CuZn nitrate solution (Cu:Zn = 70:30) were recorded at different temperatures between 30 and 60 °C and are shown in Figure 6. The titration curve obtained at 60 °C qualitatively resembles the one presented in Figure 4 obtained at slightly different conditions (higher temperature, higher metal concentrations, lower starting acidity and faster base addition, see experimental section). Again, the relevant features are gerhardite formation near pH 3 and subsequent precipitation of $Zn^{2+}$ around pH 5. This curve can, thus, be regarded as being composed of the curves observed for the single systems (Figure 1, 2). The typical features are found roughly at the same position on the abscissa, i.e. at a similar amount of base addition, but are shifted by almost a full unit on the pH scale as the temperature was decreased from 60 to 30 °C (Figure 6, inset). This up-shift is most pronounced in the temperature interval between 50 and 60 °C.

Constant pH co-precipitations were performed for the ternary CuZnAl system using nitrate and formate solutions to study the effect of the counter ion in the technically applied synthesis method. After ageing in the mother liquor the precipitates were washed and submitted to XRD measurements. The XRD patterns are shown in Figure 7. The typical phase mixture of zincian malachite and a hydrotalcite-like phase was found in the ternary samples. The crystallinity of the formate-derived precursor was extraordinary

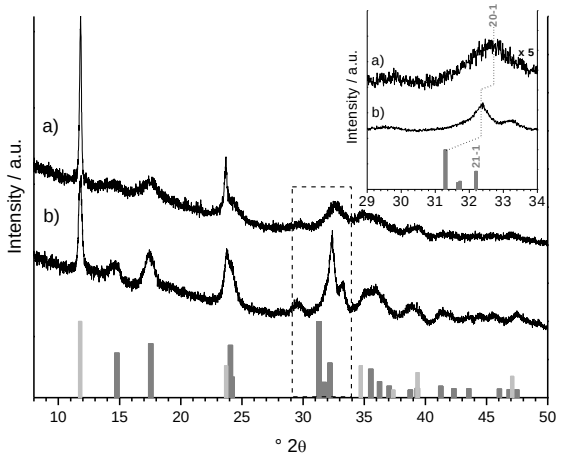


**Fig. 7:** XRD patterns of the CuZnAl precursors prepared at pH 6.5 from formate (a) and nitrate (b) solutions. The region of the 20-1 reflection of malachite is marked and shown in the inset. The bar graphs refer to hydrotalcite (light grey) and malachite (dark grey).

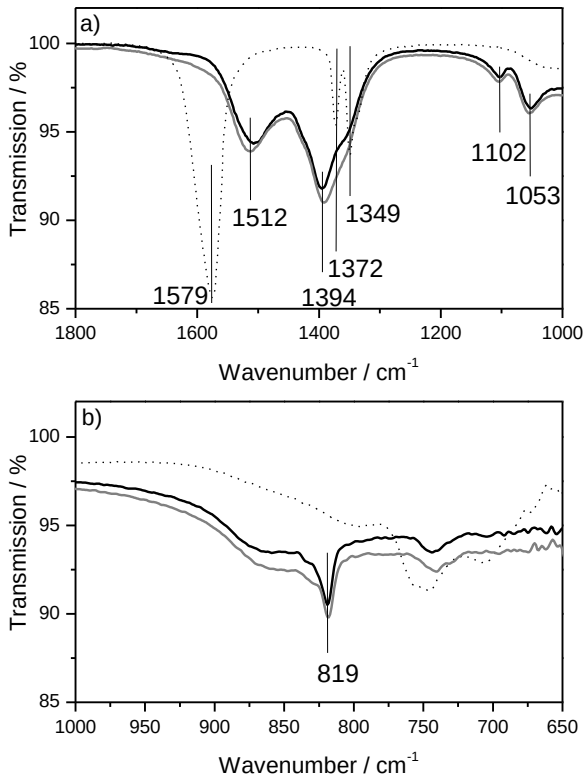


**Fig. 8:** IR spectra of samples obtained by constant pH-precipitation from nitrate solution (black), formate solution (grey) and a CuZn hydroxy formate sample (dashed) in the ranges (a) 1800–1000cm$^{-1}$ and (b) 1000–650cm$^{-1}$.

low. The position of the 20-1 reflection of the zincian malachite phase, which is indicative of the degree of Zn incorporation into this phase [28], is near 31.2 °2θ in pure malachite. For the Zn-containing precursors, a strong shift of the 20-1 reflection angles beyond 32 °2θ was observed due to the incorporation of Zn in the malachite lattice. This shift is even stronger for the formate sample compared to the nitrate one indicating a higher degree of Zn incorporation into zincian malachite. (Figure 7, inset). Due to the poor crystallinity of both samples, IR spectroscopy was applied being capable of probing both the amorphous and crystalline parts. Figure 8 shows sections of the FTIR spectra of the both samples (solid lines) and for comparison a spectra of the unknown mixed binary CuZn hydroxy formate sample was included (see section 4.2, below). The two ternary samples showed similar bands in all areas of the spectra with only faint differences in position and intensity indicating that both materials are similar not only in their long range order, but also in the local arrangement and ratio of the carbonate and hydroxyl anions, independent if they were prepared from nitrate or formate solutions. In the region of 1800 to 1000 cm$^{-1}$ (Figure 8a) the asymmetric C-O stretching mode of the carbonate anions could be observed. Both samples show four bands around 1512, 1394, 1102 and 1053 cm$^{-1}$ [28]. In the range of 1200-600 cm$^{-1}$ (Figure 8b) OH deformation vibrations and further carbonate bands can be found. The $\nu_2(CO_3^{2-})$ band at 819 cm$^{-1}$ can be related to zincian malachite or hydrotalcite for both samples.

The methanol synthesis activity at 10 bar and 220 °C as well as the gas accessible Cu surface areas ($SA_{Cu}$) were determined for the Cu/ZnO/$Al_2O_3$ catalysts derived from these two samples and selected results are summarized in Table 1. $SA_{Cu}$ were 36.9 $m^2g^{-1}$ and 36.1 $m^2g^{-1}$ for the formate and nitrate sample, respectively, which falls in the regime of industrially relevant catalysts. The productivities scaled roughly with these values and it was higher by 6 % for the formate-derived sample.

## 4. Discussion

### *4.1. Hydrolysis chemistry of the nitrate system*

From the titration curves it is directly evident that pH control during the co-precipitation of CuZnAl precursors is crucial for preparation of a homogeneous catalyst if the conventional nitrate route is used. Under uncontrolled increasing pH, i.e. if the precipitating agent is poured into the acidic metal solution, the CuZnAl system will never co-precipitate in the sense that the metal species solidify simultaneously to form a multinary material. Instead, $Cu^{2+}$ will be completely transformed into gerhardite prior to the formation of a Zn-containing compound and the desired microscopically homogeneous distribution of the metal species cannot be achieved. This problem of sequential precipitation and the step-like shape of the titration curve in the CuZn(Al) system have been reported in literature [29,30]. The influence of minor amounts of $Al^{3+}$, forming mostly amorphous precipitates in the single metal experiment, is not easily characterized solely on the basis of titration experiments, but it can be concluded by comparison of Figure 4 and Figure 5 that its presence does not generally change the sequential solidification process of $Cu^{2+}$ and $Zn^{2+}$ in the ternary titration experiment.

Although, sometimes different phases are observed in the binary and ternary nitrate system compared to the single metal systems (see supplementary data), the shape of the titration curves can always be regarded as being composed from the single metal experiments. This indicates that the solidification process is dominated by the individual hydrolysis chemistry of the different ions and that multinary compounds (like aurichalcite or zincian malachite) are formed by reactions of the fresh single metal precipitates rather than by direct co-precipitation. These processes may happen fast like in the case of aurichalcite, which readily forms from the binary solution after solidification of $Zn^{2+}$, or slowly like in the case of zincian malachite, which does only form after prolonged reaction in the mother liquor, i.e. during ageing for typically a few hours [3,13].

The unfavorable sequential hydrolysis chemistry of the mixed Cu,Zn,Al system requires application of the constant pH method. Contrary to the increasing pH method, the

constant pH method has proven to successfully yield precursors that lead to highly active catalysts of superior homogeneity and dispersion [31]. During such an experiment the acidic solution of the metal salts and the basic sodium carbonate solution are added simultaneously into a reaction vessel in a way that the average pH in the vessel remains more or less constant near neutrality. If we assume that the hydrolysis chemistry of the ionic species does not change compared to our increasing pH titration experiments, a simple picture emerges. The same pH curves are passed through, but much faster and for each single droplet in the constant pH mode instead of gradually for the whole batch in the increasing pH mode. This means, that if the microdroplet technique at constant pH is used, all $Zn^{2+}$ (and $Al^{3+}$) introduced into the reaction vessel is immediately solidified probably not exactly simultaneously but at least very close in time and space to the $Cu^{2+}$ fraction of the same microdroplet. Thereby, the system is forced to form a (quasi-)multinary precipitate by simulating a real co-precipitation despite the lack of a thermodynamically stable mixed compound under the given conditions. Accordingly, a metastable usually amorphous precipitate of zincian georgeite [27] is obtained by constant pH co-precipitation which may lower its free energy by further transformations during ageing in the mother liquor. It is an obvious advantage of the constant pH method that the element distribution in the initial precipitate will be more homogeneous compared to an increasing pH precipitation. The subsequent transformations, i.e. the formation of crystalline multinary precursor phases, especially of the important mixed zincian malachite phase [13], by dissolution/re-precipitation events will be favored over segregation in Cu- and Zn/Al- rich phases, if the starting material exhibits a homogeneous distribution of metals on a microscopic level like in zincian georgeite. Additionally, from a process-technical point of view reproducibility and scalability of the constant pH-method are superior compared to syntheses with uncontrolled pH.

The preferable pH window of a successful constant pH precipitation can be directly seen from the titration curves. The pH of the receiver solution should not be lower than pH 5 in order to guarantee complete precipitation of $Zn^{2+}$ and $Al^{3+}$, which otherwise would remain at least partially in solution. On the other hand, the pH should stay below pH 9, because in a very basic solution oxolation of basic copper precipitates into stable tenorite, CuO, is favored. Tenorite as a single metal oxide is undesired on the stage of the precursor, because mixed phases can be decomposed into much more efficient catalysts [13]. Indeed, CuZn(Al) precursors are typically co-precipitated at neutral or even slightly acidic pH [8-10].

### *4.2. The influence of the counter ion*

If formic instead of nitric acid is used during the preparation of CuZn(Al) precursors, the hydrolysis chemistry of the metal ions is drastically influenced. The absence of nitrate prevents the formation of gerhardite in the Cu system. Instead, a well-crystalline compound is formed with a previously undescribed crystal structure.

**Table 1**: Catalyst characterization and testing results, SA = surface area.

| | Nitrate-derived catalyst | Formate-derived catalyst |
|---|---|---|
| XRD-$D_{Cu}$ reduced (nm)[a] | 5.5 | 4.4 |
| $SA_{Cu}$ ($m^2g^{-1}$) | 36.1 | 36.9 |
| Productivity ($mmol_{MeOH}$ $g_{Cat}^{-1}$ $h^{-1}$) | 11.6 | 12.3 |
| Intrinsic activity ($mmol_{MeOH}$ $m_{Cu}^{-2}$ $h^{-1}$) | 0.32 | 0.33 |

[a] Domain size of Cu after reduction, determined from XRD line width

Comparison of the XRD patterns of gerhardite, $Cu_2(OH)_3NO_3$, and this new phase (Figure 9a) suggests that the two compounds may be structurally closely related. $Cu_2(OH)_3NO_3$ is the parental compound for so-called hydroxy double salts (HDS) [32] of the general composition $[(M^{2+}_{1-x},Me^{2+}_{1+x})(OH)_{3(1-y)}]+X^{n-}_{(1+3y)/n}\cdot z\ H_2O$ with M = Me = Cu, $y = 0$, X = $NO_3$, $n = -1$ and $z = 0$. HDS phases are capable of anion exchange.

Indeed, a structural model derived from the gerhardite crystal structure [33] can be successfully fitted to the XRD pattern of the Cu formate phase using Rietveld refinement (Figure 9b). Therefore, we assign this new phase as a gerhardite-analogous basic formate $Cu_2(OH)_3HCOO$ – or to a HDS phase with M = Me = Cu, $y = 0$, X = HCOO, $n = -1$ and $z = 0$. This assignment is supported by a thermogravimetric measurement of a washed sample resulting in a mass loss of 28.9 %, which is in good agreement with the theoretical weight loss of 28.7 % for the suggested composition. In addition, the CuZn hydroxy formate sample shows characteristic IR bands around 1579, 1372 and 1349 $cm^{-1}$, typically observed for formate or carboxylate groups [34] (Figure 8a, dotted lines). By comparison with the ternary mixed zincian malachite and hydrotalicte materials, it can be concluded that this sample was carbonate free. A detailed description of the crystal structure analysis will be published separately. The lattice parameters obtained from fitting of the XRD data presented in this work are summarized in Table 1. While the unit cell axes are very similar, the monoclinic angle is strongly increased from less than 95° to more than 105°, if formate instead of nitrate is crystallized.

Close inspection of the XRD patterns obtained from pure Cu and mixed CuZn solutions reveals systematic shifts of certain groups of reflections as shown in the inset of Figure 9a. The groups are shifted in opposite directions relative to the pure Cu phase. This observation indicates formation of a mixed Cu,Zn HDS phase (M = Cu, Me = Zn, $0 < x \leq 0.3$), which shows anisotropic variations of its lattice parameters as a function of Zn incorporation. The lattice parameters of this mixed $(Cu,Zn)_2(OH)_3HCOO$ phase obtained from XRD fitting are also included in Table 2.

a)

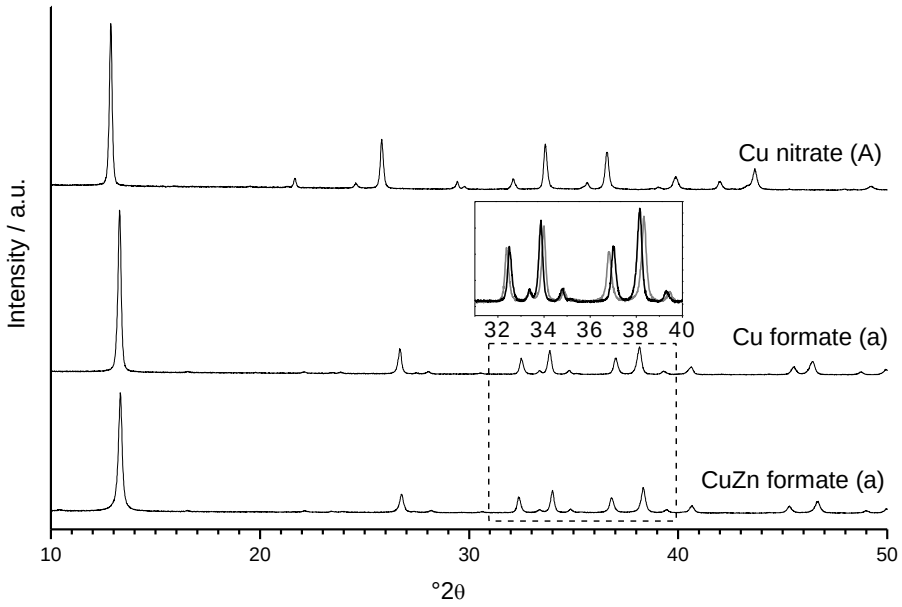


b)

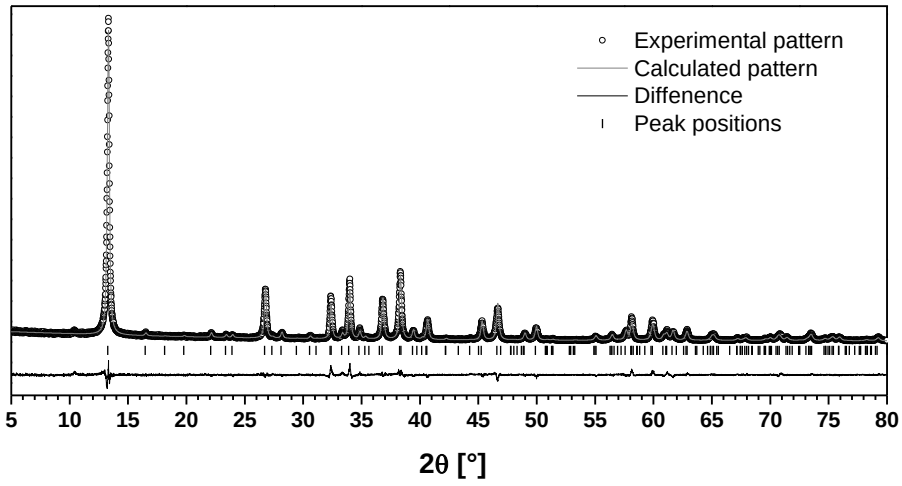


**Fig. 9:** Comparison of the XRD patterns of the samples obtained from Cu nitrate at point A (pure gerhardtite), from Cu formate at point a in Fig. 1 and from CuZn formate at point a in Fig. 4 (a). Rietveld plot of basic Cu formate recovered at point a in Fig. 1 using the gerhardite crystal structure as model (b).

**Table 2**: Lattice parameters of gerhardite $Cu_2(OH)_3NO_3$ and the new basic formates $(Cu,Zn)_2(OH)_3HCOO$ (see text). All values are strongly rounded to a common digit for convenient comparison. The letters in parentheses refer to the points of sample recovery as indicated in Figure 1 and 4.

| | Gerhardtite | Cu formate (Figure 1 & S1b) | | | Cu,Zn formate (Figure 4 & S4b) | |
|---|---|---|---|---|---|---|
| | ref. [33] | *(a)* | *(b)* | *(c)* | *(a)* | *(b)* |
| *a* [Å] | 5.60 | 5.60 | 5.59 | 5.59 | 5.57 | 5.58 |
| *b* [Å] | 6.08 | 6.07 | 6.07 | 6.07 | 6.10 | 6.09 |
| *c* [Å] | 6.93 | 6.94 | 6.94 | 6.94 | 6.94 | 6.94 |
| $\beta$ [°] | 94.6 | 105.9 | 105.8 | 105.9 | 105.3 | 105.3 |

The structural variations are only small, as could be expected from the similar ionic radii of $Cu^{2+}$ and $Zn^{2+}$. In detail, the *a*-axis and the monoclinic angle seem to be slightly contracted, while the *b*-axis is increased and the *c*-axis remains almost constant as a function of Zn incorporation. No significant differences are observed for the precipitates obtained at point *a* and *b* during the titration experiment of the mixed formate solution (cf. Figure S4b). It is noted that a discontinuous series of solid solutions was reported for the hydrated form of Cu,Zn formate, $(Cu,Zn)(HCOO)_2 \cdot 2\ H_2O$ [35], for which some axes were also observed to be shifted into opposite directions with Cu-Zn substitution. Such mixed Cu,Zn compounds with decomposable anions are promising candidates for preparation of highly dispersed Cu/ZnO catalysts and a detailed investigation of the crystal structure and the cation composition of the novel $(Cu,Zn)_2(OH)_3HCOO$ phase as well as its potential as catalyst precursor will be reported elsewhere.

In general, it can be estimated on the basis of the shape of the titration curves, that the problem of sequential hydrolysis of the cations at different pH, which prevents easy formation of a homogeneous co-precipitate in the nitrate system, is less severe for the formate system. Due to the absence of gerhardtite, the onsets of precipitation of the three single components occur all in a relatively narrow regime between pH 5 and 6. Furthermore, the typical step-like shape, which is indicative of the sequential solidification of the single components, is not observed in the curves of the mixed formate solutions. The smoother evolution of pH may be explained with the characteristics of the formate anions. Firstly, the contribution to acid-base chemistry is much larger for formate anions compared to nitrate (Scheme 1). Secondly, the lower dissociation constant of Cu(II) formate compared to nitrate [36] and the complexing power of the formate ion suggests the presence of species like $[Cu(HCOO)_2]$, $[Cu(HCOO)]^+$ [37] or $[Cu_2(HCOO)_4]$ [38] in concentrated solutions. Thus, formate may acts as a protecting ligand for the copper ions. Therefore, precipitation of basic salts from a formate solution involves additional acid-base- and complex formation equilibria. The coupling of these three events – buffering, ligand exchange and precipitation – represents a strong and complicated modification of the hydrolysis chemistry of the metal cations. Apparently, the situation favors a gradual and simultaneous rather than a sequential precipitation of the different metal species, which is beneficial for the homogeneity of the metal distribution in the precipitate.

As a result of the modified hydrolysis, a significantly larger amount of Zn can be incorporated into the zincian malachite phase formed upon ageing if it is prepared from formate solutions compared to nitrate solutions using constant pH co-precipitation. This is indicated by the extraordinary strong shift of the 20-1 reflection of the zincian malachite phase [28]. This phase was identified as the relevant precursor phase for technically applied Cu/ZnO-based methanol synthesis catalysts, in which a large degree of Zn incorporation is generally desired. The reason is that such materials, which exhibit a more homogeneous cation distribution, can be decomposed to more efficient catalysts [13]. Indeed, the MeOH productivity of the formate derived sample is superior in our catalytic test compared to the conventional nitrate-based sample. The larger gas accessible Cu surface area can be explained as a result of more effective nano-structuring of the Zn-richer zincian malachite precursor, while also the intrinsic activity (normalized to $SA_{Cu}$) is slightly higher (Tab. 1). The reason for the superior Zn incorporation may lie in the modified hydrolysis chemistry during precipitation due to the presence of formate anions as discussed above. It is noted, however, that the presence of formate anions will not only change the hydrolysis chemistry during solidification, but may also influence the dissolution/re-precipitation events happening during phase formation upon ageing and, thus, also strongly affect the crystallinity and morphology of the precursor material (Figure 7).

### *4.3. The effect of temperature in the nitrate system*

As seen in Figure 6 an increase of temperature of co-precipitation leads to a shift of the titration curves to lower pH values confirming that the proper selection of temperature and pH is crucial for the complete solidification of all components. A direct consequence is that reduction of temperature at the same precipitation pH may lead to incomplete solidification of $Zn^{2+}$ by shifting the Zn precipitation plateau below the applied pH. In turn, elevation of temperature enables complete solidification at a more acidic pH. The beneficial effect of neutral or slightly acidic pH during preparation is obvious from the study of Baltes et al. [10]. Their Figure 2 impressively illustrates the chemical memory of the CuZnAl system and the important role of precursor chemistry. It shows the methanol synthesis activity of a large set of Cu/ZnO/$Al_2O_3$ samples of the same starting composition prepared at different conditions as a function of pH and temperature. Enormous differences were observed and a relatively sharp maximum was found for $6 < pH < 7$ and $60 < T < 70$ °C.

The lower limit of acidity is clearly given by the pH of $Zn^{2+}$ precipitation. This seems to be a quite sharp limit as can be seen from the rapid breakdown of activity observed by Baltes et al. if the precursor is prepared at a $pH < 6.5$. To guarantee a full solidification in the favorable pH range near neutrality, the critical Zn precipitation plateau has to be shifted to lower pH by increasing the temperature > 60 °C (Figure 6). The higher limit of the precipitation temperature, however, is given by the sensitivity of the initial basic Cu precipitate towards formation of CuO by oxolation, because the dehydration rate $Cu(OH)_2$ increases in the presence of alkali and with temperature.

Lowering the temperature at optimal pH near 6.5 consequently also leads to a breakdown of activity. The

detrimental effects of too low pH and temperature may, thus, be explained in both cases by a suboptimal nanostructuring of such material due to a lack of Zn in precursor. One promoting effect of Zn is that it serves as a stabilizing geometrical spacer in form of ZnO nanoparticles between active Cu particles in the final catalyst preventing sintering. This function of ZnO is most effective, if large amounts of the Zn-fraction are incorporated into the zincian malachite precursor phase [13]. In line with this interpretation, Baltes et al. observed a lack of Zn in the precipitate for samples prepared at pH < 6 and T < 50 °C compared to the concentrations of the starting solution indicating incomplete solidification of $Zn^{2+}$ under these conditions. This lack of Zn was associated with a breakdown of activity in methanol synthesis.

Temperature and pH of precipitation, thus, has to be high enough to avoid a lack of Zn in the precipitate, but low enough not to enter the basic regime and to avoid partial oxolation of $Cu^{2+}$. Apparently, conditions near pH 6.5 and 65 °C represent the best balance of these effects for preparation of Cu/ZnO/$Al_2O_3$ catalysts.

## 5. Conclusion

For preparation of Cu/ZnO/$Al_2O_3$ catalysts by co-precipitation using the conventional nitrate route, a micro-droplet technique at constant pH is required due to the sequential hydrolysis of $Cu^{2+}$ and $Zn^{2+}$, which prevents homogeneous distribution of both species in the precipitate. The key for preparation of effective Cu/ZnO/($Al_2O_3$) catalysts is the incorporation of Zn into the zincian malachite precursor phase. The right level of acidity during co-precipitation and ageing is critical for this process because at too low pH some Zn is not solidified, remains in the mother liquor and cannot be incorporation into zincian malachite. The optimal acidity seems to be the lowest possible pH, which still guarantees a complete solidification of $Zn^{2+}$. It can be realized by increasing the temperature, but the tendency of the initial Cu precipitate towards oxolation sets a limit for temperature elevation. On the basis of these considerations, the empirically determined optimal pH and temperature conditions of the industrially applied synthesis can be rationalized, showing the complexity of the CuZn(Al) co-precipitation system as well as its already highly optimized character.

The presence of other counter ions can drastically change the hydrolysis chemistry of the components and lead to new approaches of preparation or even further optimization. Formate-derived precursors are a promising example, which (even if prepared under conditions optimized for the nitrate system) lead to a higher Zn content of the zincian malachite precursor phase and a more homogeneous metal distribution of Cu and Zn in the final catalyst. This is reflected in higher activity due to a larger Cu surface area.

Moreover, a new basic formate $(Cu,Zn)_2(OH)_3(HCOO)$ was prepared and its crystal structure preliminarily characterized. This material is a promising new precursor phase for Cu/ZnO catalysts and will be subject to further investigations.

### Acknowledgements

This paper has emerged from a joint research project “Next generation methanol synthesis catalysts” with the partners Süd-Chemie AG (Bruckmühl, Germany), Fritz-Haber-Institute (Berlin, Germany), Ruhr-University Bochum (Germany) and NanoC (Kuala Lumpur, Malaysia), which was funded by the German Federal Ministry of Education and Research (BMBF, FKZ 01RI0529). Edith Kitzelmann (XRD) and Gisela Lorenz (BET) and Jutta Kröhnert (IR) are acknowledged for their help with sample characterization.

### References

[1] F. Schüth, M. Hesse, K. K. Unger, in: G. Ertl, H. Knözinger, F. Schüth, J. Weitkamp (Eds.), Handbook of Heterogenous Catalysis Vol. 2, Wiley-VCH, Weinheim, pp. 100-119.
[2] S. Schimpf, M. Muhler, in: Krijn de Jong (Ed), Synthesis of Solid Catalysts, Wiley-VCH, Weinheim, pp. 329-351.
[3] B. Bems, M. Schur, A. Dassenoy, H. Junkes, D. Herein, R. Schlögl, Chem. Eur. J. 9 (2003) 2039-2052.
[4] G. J. Millar, I. H. Holm, P. J. R. Uwins, J. Drennan, J. Chem. Soc. Faraday Trans. 94 (1998) 593-600.
[5] P. Porta, G. Fierro, M. Lo Jancono, G. Moretti, Catal. Today 2 (1988) 675-683.
[6] P. B. Himmelfarb, G. W. Simmons, K. Klier, R. G. Herman, J. Catal. 93 (1985) 442-450.
[7] G. C. Shen, S.-I. Fujita, N. Takezawa, J. Catal. 138 (1992) 754-758.
[8] J.-L. Li, T. Inui, Appl. Cat. A 137 (1996) 105-117.
[9] D. Waller, D. Stirling, F. S. Stone, M. S. Spencer, Faraday Dissuss. Chem. Soc. 87 (1989) 107-120.
[10] C. Baltes, S. Vukojevic, F. Schüth, J. Catal. 258 (2008) 334-344.
[11] M. Schneider, K. Kochloefl, J. Ladebeck; Patent DE3317725 A1, 1984
[12] S. Polier, M. Hieke, D. Hinze; Patent WO2006117190 A1, 2006
[13] M. Behrens; J. Catal. 267 (2009) 24-29.
[14] EVA version 9, copyright 1996-2003, SOCABIM
[15] TOPAS version 3, copyright 1999, 2000, Bruker AXS
[16] O. Hinrichsen, T. Genger, M. Muhler, Chem. Eng. Technol. 23 (2000) 956-959.
[17] G. C. Chinchen, C. M. Hay, H. D. Vanderwell, K. C. Waugh, J. Catal. 103 (1987) 79-86.

[18] J. W. Geus, A. J. van Dillen, in: G. Ertl, H. Knözinger, F. Schüth, J. Weitkamp (Eds), Handbook of Heterogenous Catalysis Vol. 2, Wiley-VCH, Weinheim, pp. 428-467.
[19] B. Bems, Ph.D. Thesis, Technical University Berlin, 2003.
[20] G. Fowles, J. Chem. Soc. 107 (1915) 1281.
[21] V. Kohlschütter, M. Christen, F. Rinne, Helv. Chim. Acta 17 (1934) 1094-1119.
[22] C. C. Perry, K. L. Shafran, J. Inorg. Biochem. 87 (2001) 115-124.
[23] A. C. Vermeulen, J. W. Geus, R. J. Stol, P. L. de Bruyn, J. Colloid Interface Sci. 51 (1975) 449-458.
[24] J. J. Fitzgerald, L. E. Johnson, J. S. Frye, J. Magn. Reson. 84 (1989) 121-133.
[25] B. C. Faust, W. B. Labiosa, K'o H. Dai, J. S. MacFall, B. A. Browne, A. A. Ribeiro, D. D. Richter, Geochim. Cosmochim. Acta 59 (1995) 2651-2661.
[26] S. L. Wang, M. K. Wang, Y. M. Tzou, Colloids Surf. A 231 (2003) 143-157.
[27] A. M. Pollard, M. S. Spencer, R. G. Thomas, P. A. Williams, J. Holt, J. R. Jennings, Appl. Catal. A 85 (1992) 1-11.
[28] M. Behrens, F. Girgsdies, A. Trunschke, R.Schlögl, Eur. J. Inorg. Chem. 10 (2009) 1347-1357.
[29] P. Coutry, C. Marcilly, in: G. Poncelet, P. Grange, P. A. Jacobs (EDs), Preparation of Catalysts III, Elsevier, Amsterdam, 1983, pp. 485-520.
[30] C. Perego, P. Villa, Catal. Today 34 (1997) 281-305.
[31] M. S. Spencer, Top. Catal. 8, (1999) 259-266.
[32] M. Meyn, K. Beneke, G. Lagaly, Inorg. Chem. 32 (1993) 1209-1215.
[33] N. Guillou, M. Louër, D. Louër, J. Solid State Chem. 109 (1994) 307-314.
[34] Y. Koruda, M. Kobu, Spectroch. Acta Part A, Mol. Biomol. Spec, 23 (1967) 2779-2789.
[35] D. Stoilova, G. Gencheva, J. Solid State Chem. 100 (1992) 24-29.
[36] E. H. E. Pietsch, A. Kotowski (ed.) in: Kupfer – Teil B 176, Gmelin Institut für Anorganische Chemie, Verlag Chemie, Weinheim, 1958, pp. 671-685.
[37] A. Günther-Schulze, Z. Elektrochem. 28 (1922) 89-99.
[38] R. L. Martin, H. Waterman, J. Chem. Soc. 6 (**1959)** 1359-1370.